Origin and Consequences of Steric Strain in the Rhodopsin Binding Pocket†

Minoru Sugihara,*,‡,§ Julia Hufen,§ and Volker Buss§

Institute of Theoretical Low-Temperature Physics and Institute of Theoretical Chemistry, University of Duisburg-Essen, 47057 Duisburg, Germany

Received August 5, 2005; Revised Manuscript Received October 7, 2005

ABSTRACT: To study the origin and the effects of steric strain on the chromophore conformation in rhodopsin, we have performed quantum-mechanical calculations on the wild-type retinal chromophore and four retinal derivatives, 13-demethyl-, 10-methyl-13-demethyl-, 10-methyl-, and 9-demethylretinal. For the dynamics of the whole protein, a combined quantum mechanics/molecular mechanics method (DFTB/CHARMM) was used and for the calculation of excited-state properties the nonempirical CASSCF/CASPT2 method. After relaxation inside the protein, all chromophores show significant nonplanar distortions from C10 to C13, most strongly for 10-methylretinal and least pronounced for 9-demethylretinal. In all five cases, the dihedral angle of the C10−C11═C12−C13 bond is negative which attests to the strong chiral discrimination exerted by the protein pocket. The calculations show that the nonplanar distortion of the chromophore, including the sense of rotation, is caused by a combination of two effects: the fitting of both ends to the protein matrix which imposes a distance constraint and the bonding arrangement at the Schiff base terminus. With both the counterion Glu113 and Lys296 displaced off the plane of the chromophore, their binding to N16 exerts a torque on the chromophore. As a result, the polyene chain, from N16 to C13, is twisted in a clockwise manner against the remaining part of the chromophore, leading to a C11═C12 bond with the observed negative dihedral angle. Shifts of the absorption maxima are reproduced correctly, in particular, the red shift of the 10-methyl and the strong blue shift of the 9-demethyl analogue relative to the wild type. Calculated positive rotatory strengths of the α-CD bands are in agreement with the calculated absolute conformation of the mutant chromophores.

Rhodopsin is the visual pigment that mediates light−dark vision in the vertebrate eye. It is a prototypical G-protein-coupled receptor (GPCR),[1] a superclass of membrane proteins which are responsible for signal transduction in mammalian cells. Involved in a broad range of body functions and processes and related to major diseases, they constitute one of the most important groups for drug targeting (*1*, *2*). All GPCRs share the structural feature of seven transmembrane helices connected by six outer membrane loops. Like all membrane proteins, they are difficult to crystallize, and despite an enormous interest in their structure and function, no high-resolution structure of any GPCR was known until only 5 years ago. This changed when a way to stabilize rhodopsin in the crystalline state in the presence of high concentrations of zinc ions was found (*3*). There are now five structures of the rhodopsin dark state deposited with the Protein Data Bank (*4*−*8*), the last one with a resolution of 2.2 Å, which reveal the structure of the protein including the chromophore in remarkable detail.

The chromophore of rhodopsin is 11-*cis*-retinal which is embedded in a pocket formed by 27 amino acids within 4.5 Å of the chromophore (*4*). It is linked as a protonated Schiff base (pSb) to the side chain of Lys296 at helix 7; this position is additionally stabilized by a salt bridge involving Glu113 and a hydrogen bond network involving several polar side chains and two water molecules (*7*, *9*). The *β*-ionone terminus is enclosed (*10*) in a hydrophobic pocket formed by aromatic residues around Pro267 in helix 6. One consequence of protonation is the broad absorption in the visible wavelength range with a maximum at 500 nm (*11*). In the dark state, the chromophore acts as an antagonist toward G-protein coupling, stabilizing the inactive state of rhodopsin and making it extremely inactive against thermal activation (*12*). Photoisomerization of the chromophore from 11-cis to all-trans initiates a sequence of events (*13*) which at the deprotonated metarhodopsin II state triggers the G-protein cascade, resulting in the closing of sodium channels and excitation of the visual nerve (*14*).

The conformation of the chromophore inside the binding pocket is 6-s-cis-11-cis-12-s-trans-15-16-anti; this is the combined result of spectroscopic methods, in particular, nuclear magnetic resonance (NMR) (*15*−*18*), resonance Raman (RR) (*19*, *20*), and circular dichroism (CD) spec-

† This work was supported by the Research Group on Molecular Mechanisms of Retinal Protein Action and by the Graduate College on Structure and Dynamics of Heterogeneous Systems, both financed by the German Research Council.

* To whom correspondence should be addressed. Phone: +49-203-3791073. Fax: +49-203-3793665. E-mail: minoru@thp.uni-duisburg.de.

‡ Institute of Theoretical Low-Temperature Physics.

§ Institute of Theoretical Chemistry.

[1] Abbreviations: ANO, atomic natural orbital; CAS, complete active space; CASSCF, CAS self-consistent field; CD, circular dichroism; CASPT2, CAS second-order perturbation theory; DFT, density functional theory; FTIR, Fourier transform infrared; GPCR, G-protein-coupled receptor; MD, molecular dynamics; NMR, nuclear magnetic resonance; pSb, protonated Schiff base; QM/MM, quantum mechanics/molecular mechanics; RR, resonance Raman; SCC-DFTB, self-consistent-charge density-functional tight binding; 9dm, 9-demethyl; 10me, 10-methyl; 10me,13dm, 10-methyl-13-demethyl; 13dm, 13-demethyl.

10.1021/bi0515624 CCC: $33.50
Published on Web 12/21/2005

troscopy (*21*, *22*). The retinal chain is significantly twisted about the C6−C7 single bond, a consequence of internal steric interaction between the C5 methyl group and the C8 hydrogen. There is another area of nonplanar distortion involving the three bonds from C10 to C13. This distortion results from steric interaction of the chromophore with the binding pocket, since the isolated chromophore is essentially planar in that region (*23*, *24*). There are indications from experiment that this torsion is a prerequisite for the extremely fast, selective, and efficient photoreaction of rhodopsin. In 13-demethylrhodopsin (13dm-rhodopsin), the photoreaction is slowed (*25*) and the quantum yield is reduced significantly (*22*, *26*). In 10-methyl-13-demethylrhodopsin (10me,13dm-rhodopsin) in which the methyl group is reintroduced in the C10 position, the quantum yield almost returns to the original value (*27*). These results support the hypothesis that the nonplanar distortion about the C11═C12 bond should give rise to high initial torsional velocity as the chromophore moves out of the Franck−Condon region after photoexcitation (*28*). There are experimental data for two more rhodopsins which differ in the methyl substitution pattern of their chromophore from the wild type: 10-methylrhodopsin (10me-rhodopsin), which despite its strongly twisted geometry slows the kinetics of the rhodopsin photocascade (*29*), and 9-demethylrhodopsin (9dm-rhodopsin), which inhibits light-dependent activation of the G-protein (*30*).

This study focuses on the following questions: What is the mechanism which induces the peculiar geometry of retinal, in particular, the twists about the C11═C12 bond and the C12−C13 bond of the polyene chain which seem to be crucial for the fast photokinetics of rhodopsin? Further, which are the factors that determine the absolute conformation of the chromophore in this twisted area and thereby determine the physical path that the chromophore will follow after photoexcitation? Finally, do the calculated UV−vis and CD spectroscopic properties agree with the proposed structures of rhodopsin and the rhodopsin analogues? These questions imply that the model we have chosen, treatment of the chromophore by quantum mechanics and of the protein environment by classical force-field theory, is of sufficient quality to adequately describe this enormously complex system. The purpose of the comparative study involving the retinal analogues is to test this assumption and see whether the structures and excited-state properties obtained with our model yield a description which is consistent with experimental evidence.

MODELS AND METHODS

Models. Molecular models of rhodopsin and of rhodopsin mutants were constructed on the basis of the coordinates of chain A of the refined crystal structure of Okada (*6*) (PDB entry 1L9H); missing residues 236−240 and 331−333 were inserted and optimized using the CHARMM force field (*31*). Several molecules which bind covalently to rhodopsin and adhering molecules were not included. Metal ions were replaced with water molecules, resulting in 15 water molecules in total, two of them in the retinal binding pocket. The size of the entire system (including the chromophore) was 5577 atoms. All titratable groups were assumed to be charged except for the histidine residues, Asp83, Glu122, and Glu181. As a result, the binding pocket is neutral, and the whole protein has a charge of −1. Chromophores and their numbering are shown in Chart 1.

Chart 1: Structural Formulas and Atom Numbering of the Wild-Type Chromophore and of the Four Analogues Studied in This Work

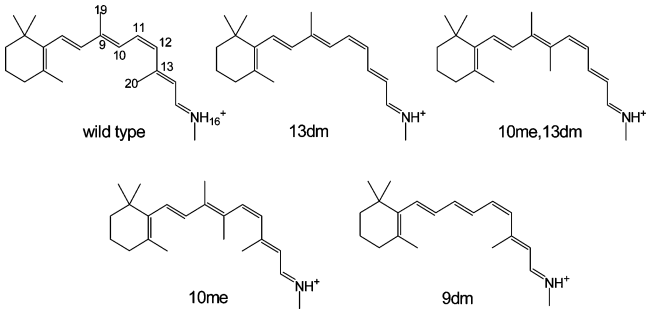

In a previous ab initio molecular dynamics (MD) simulation, it was observed that Thr94 forms a hydrogen bond with one of the oxygen atoms of Glu113 (*9*). This bond is critical for stabilizing the salt bridge (*32*); however, it is not evidenced in any of the structure analyses. Independently, Crozier et al. have performed a 40 ns MD simulation of rhodopsin and found that after simulation for 10 ns residues Ser186 and Thr94 start to coordinate with Glu113 (*33*). In accordance with these results, we brought the polar side groups of these amino acids into the proper orientation to make a hydrogen bond with one of the carboxyl oxygen atom (Oϵ2) of Glu113. The detailed setup of the model is described elsewhere (*8*).

Methods. Structures were calculated with embedded quantum chemistry (QM/MM) using the SCC-DFTB and CHARMM codes (*34*), which has been successfully applied before to retinal proteins (*8*, *35*, *36*). The QM region consisted of the chromophore, Lys296, Glu113, Thr94, and a water molecule, wat2b (85 atoms, including the link atoms). Wat2b makes a direct hydrogen bond with the counterion and stabilizes the protonation state of the chromophore (*9*, *32*). Link atoms were added to the borderline amino acids: C_γ of Lys296 and C_β of Glu113 and Thr94. All other atoms were treated with the CHARMM force field with parameter set 22 (*31*). Except for 111 amino residues next to the chromophore, they were given harmonic constraints to retain the shape of the protein. A 12 Å cutoff value was used for nonbonding interaction, and the time step was 1 fs.

Each model was heated at constant pressure to 300 K and followed for 200 ps using the Nose algorithm (*37*). Ten configurations were selected at random and used as starting geometries for the statistics. They were each heated to 300 K and their dynamics followed for 200 ps in the manner described above; two of the 10 MD trajectories were continued for up to 1 ns to confirm the stability of the model. Each of the final MD structures was then subjected to geometry minimization inside the protein pocket. The resulting structures turned out to be essentially identical. Internal coordinates and their error margins for the 10 MD runs and the 10 optimized structures are listed for each of the five models in the Supporting Information. Also given for each model are the Cartesian coordinates on which the electronic structure calculations were based.

For the calculation of ground- and excited-state energies, we employed the CASSCF/CASPT2 method as provided by the MOLCAS5 set of routines (*38*). In short, CASSCF

computes an ab initio multiconfigurational wave function in an atomic natural orbital (ANO) set consisting of 4s3p1d for carbon and nitrogen and 2s for hydrogen. The active space included all valence π-electrons and as many orbitals. Corrections to the CASSCF energies were obtained with CASPT2 which performs second-order perturbation theory for specified states. CASPT2 energies were combined with transition dipole moments calculated by the CAS-state interaction method (*39*) to obtain oscillatory and rotatory strengths. The method is very time-consuming; therefore, the chromophores were reduced to five-double bond systems by omitting the β-ionone ring, and the counterion was reduced to the formiate anion $HCOO^-$ and wat2b. The CASSCF/CASPT2 method has been successfully applied elsewhere to calculate the spectroscopic properties of the retinal chromophore (*40*−*43*). A critical evaluation of CASPT2 relative to other theoretical methods has appeared recently (*44*).

RESULTS AND DISCUSSION

Geometries. We start by first discussing the chromophores before they interact with the protein. Figure 1 shows the internal coordinates of the five retinals as pSb but without counterion after energy minimization in the gas phase. Substitution of hydrogen with a methyl group is seen to affect mainly the bond lengths and bond angles next to this group: Bond lengths increase by 0.15−0.2 Å, and bond angles opposite to the methyl group are compressed by ∼5°. Both effects are a consequence of the increased size of the substituent.

Note that a methyl group in the 10-position is needed to induce nonplanarity in the chromophore chain (Figure 1, bottom panel). Only the 10me,13dm- and 10me-retinal pSb are significantly twisted about the C11−C12 bond, by 16° and 31°, respectively. This effect is caused by the 9-methyl group (Figure 2): Space for this group is made by opening the CH3−C9−C8 and CH3−C9−C10 bond angles, which in turn forces the hydrogens at C8 and C10 against each other. Substitution of the C10 hydrogen with methyl has the same effect on the two hydrogens at C9 and C11, and this compound (it would be a model chromophore for 9,13-demethyl-10-methylretinal which is not a subject of this study) is essentially planar, with a calculated C11═C12 torsion angle of 4°. Only when both C9 and C10 are substituted with methyl groups is the inward movement of the two opposite substituents impeded, and the chromophore reduces the steric strain instead by concerted rotation about the C10−C11 and C11═C12 bonds.

The same argument applies to the C13 methyl group which is often, and wrongly, held responsible for the nonplanar distortion of the chromophore in rhodopsin due to nonbonded interaction with the C10 hydrogen. As Figure 1 shows, the polyene chain of the wild-type chromophore is essentially planar in accordance with the results of more sophisticated computations (*23*, *24*).

For the two strongly twisted species, the 10me,13dm- and 10me-retinal pSb, Figure 1 presents two conformations with opposite twists along the conjugated chain. In the absence of other chiral elements, these conformations are mirror images and cannot be distinguished. The nonplanar β-ionone ring differentiates between these two conformations, strongly

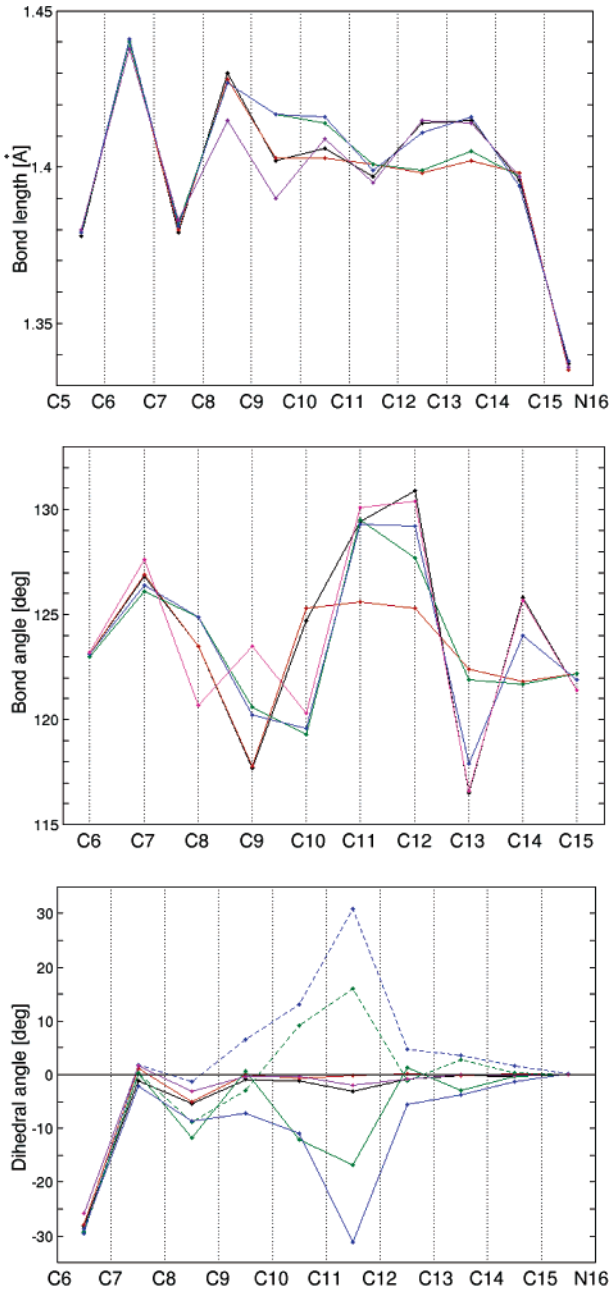

FIGURE 1: Internal coordinates of the protonated Schiff bases of retinal and of retinal analogues optimized outside the protein binding pocket. The dihedral angles indicate the deviations from planar cis (0°) or planar trans (180°). The dotted lines indicate optimized structures which were generated starting with a positive C11═C12 dihedral angle. The color code is as follows: black for wild type, red for 13dm, green for 10me,13dm, blue for 10me, and magenta for 9dm.

from C7 to C9 and not so strongly from C10 on when they begin to exhibit almost perfect mirror symmetry. Note that we have only considered conformations with negative dihedral angles about the C6−C7 bond. Their mirror images or enantiomers with positive C6−C7 dihedrals are not shown because outside the protein pocket they have identical properties.

Binding by the protein (Figure 3) reduces the differences between the chromophores significantly, making them all structurally alike. The extent of bond length alternation increases strongly, a consequence of the counterion which localizes the positive charge of the chromophore on N16 (*45*).

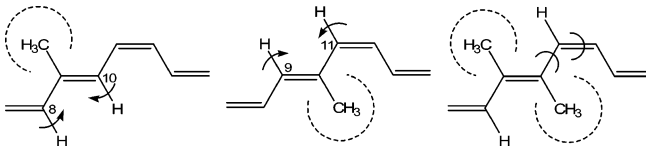

FIGURE 2: Consequences of steric strain due to methyl substitution in the retinal chromophore. At the left, the 9-methyl group enforces a close approach of the hydrogens at C8 and C10. The middle panel is the same with respect to a methyl group at the 10 position and the hydrogens at C9 and C11. At the right, with both the 9 and the 10 position substituted with methyl groups, steric strain cannot be relieved by compressing the two opposite substituents; instead, it is relieved by torsion about the C10−C11 and C11−C12 bonds.

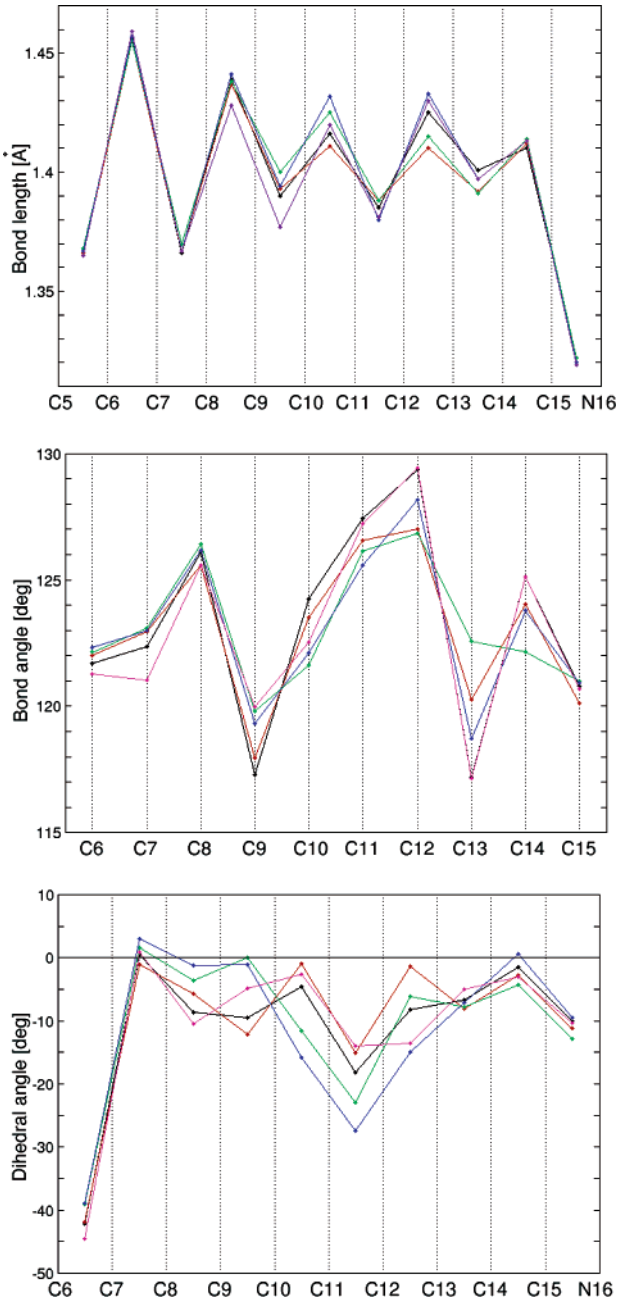

FIGURE 3: Internal coordinates of retinal and retinal analogues after relaxation inside the protein pocket. The definition of the dihedral angles and color code are as in Figure 1.

The effects of methyl substitution at C9 and C13 on the bond lengths are still visible, though reduced in magnitude. There is a clear pattern of bond angles in the pocket, and all chromophores adhere to it. Note in particular how the demethylated chromophores 13dm and 9dm with their irregular behavior at C8, C9, and C13 show bond angles similar to the others once they are inside the binding pocket.

The largest differences between the bare and protein-bound chromophores are observed in the dihedral angles. This is not surprising considering that bond rotation requires 1 order of magnitude less energy than bond stretching or bending. All chromophores are twisted about the C11═C12 cis bond which because of steric interaction between the C10 and C13 positions is prone to such a distortion. However, there is again the leveling effect of the pocket: regardless of whether they are inherently planar or strongly distorted, inside the binding pocket all chromophores are twisted about the C11═C12 bond in the narrow range between −15° and −26°, obviously to improve the fit with the pocket. A somewhat smaller angle, −6°, was found by Ferre and Olivucci (*42*), who minimized a model of the 9dm-rhodopsin without the β-ionone ring in rhodopsin.

In a study published (*46*) before the first X-ray structures of rhodopsin became available, we mimicked the strain imposed on the chromophore by the protein pocket in a crude model. We reduced the distance between the ends of the chromophore and then performed molecular dynamics calculations with the ends fixed; i.e., we followed how the system would equilibrate under this distance constraint. What happened was that the chromophore remained essentially planar from C7 to C12 and from C13 to N16, while the C11═C12 and C12−C13 bonds started to rotate in a synchronous manner, resulting in a locally twisted structure remarkable similar to one proposed earlier on the basis of NMR distance measurements (*47*, *48*). The 13dm chromophore did not twist under these same conditions (*49*). We concluded that the twisted 11-cis chromophore does not require a specific protein interaction site; rather, it is a consequence of the inherent tendency of the chromophore to twist about these bonds under the external constraints of the two end groups rigidly "anchored" in the protein (*50*), the β-ionone within its hydrophobic pocket and the Schiff base terminus by the formation of the salt bridge. About the underlying reasons, in particular, the factors which determine the direction in which the bonds rotate, we could say nothing. Today, with the geometry of the protein pocket known in atomic detail, the situation is different, and we can search with more confidence for the factors which determine the sense of twist of the chromophore.

To this end, we have performed two sets of calculations. To analyze the effect of single amino acids on the chromophore conformation, we first completely removed the protein environment and fixed the coordinates of C6 and N16, much like in the experiment described above. We then took selected groups from the environment and fixed them relative to the chromophore in the position found in the pocket. In the case of amino acids, only the backbone atoms were fixed. Then the chromophore was re-optimized under the distance constraint and the constraints imposed by the added groups. In the second set of experiments, we introduced mutations at key amino acids to see whether the conclusions reached in the first set of calculations could be substantiated. The results are summarized in Tables 1 and 2.

Table 1: Calculated C10−C11═C12−C13 and C11═C12−C13═C14 Dihedral Angles (in degrees) of the Chromophores Optimized with Constraints Due to the Binding Pocket[a]

		constraints						
	bond	C6, N16	C6, N16, C19[b]	C6, N16, Trp265, Ala117	C6, N16, H16	C6, N16, Lys296	C6, Lys296	complete pocket
13dm	C11═C12	−2.2	−1.1	−1.0	−11.7	−11.7	−10.2	−15.0
	C12−C13	178.7	−179.9	177.3	178.5	−179.2	−179.3	178.7
wild type	C11═C12	−14.4	−12.7	−14.8	−18.7	−19.3	−17.2	−18.2
	C12−C13	174.0	172.0	175.4	172.9	172.9	177.0	171.8
10me,13dm	C11═C12	−17.6	−18.8	−18.3	−21.9	−21.5	−20.9	−22.9
	C12−C13	179.8	178.1	176.5	173.7	179.1	179.1	173.9
10me	C11═C12	−28.6	−30.0	−29.8	−28.5	−29.3	−30.4	−27.4
	C12−C13	164.8	165.3	165.0	165.0	165.0	170.7	165.1
9dm	C11═C12	−15.5	−16.1	−16.2	−18.3	−18.0	−16.0	−14.0
	C12−C13	170.2	170.1	172.1	168.5	167.7	174.2	166.5

[a] Data for the complete pocket are also given. Constraints were applied by fixing in space the coordinates of the atoms or the backbone atoms of the given amino atoms. [b] In this case, Thr118, Ile189, Tyr191, Met207, and Tyr268 were constrained, but not C19.

Table 2: Effect of Point Mutations on the Calculated C10−C11═C12−C13 and C11═C12−C13═C14 Dihedral Angles (in degrees) of the 13dm and Wild-Type Chromophores[a]

	bond	E113A	K296A	E113A/K296A	A117G	W265A	A117G/W265A	wild type
13dm	C11═C12	−18.6	−11.5	−8.7	−15.6	−14.5	−15.0	−15.0
	C12−C13	−179.6	−179.4	−179.1	−177.5	−179.8	−177.5	178.7
wild type	C11═C12	−29.6	−16.7	−23.3	−19.9	−17.3	−18.2	−18.2
	C12−C13	176.6	171.8	171.6	173.8	173.2	175.6	171.8

[a] Data for the wild-type pocket are also given.

Turning to Table 1, we first see that when only the distance constraint is applied (first column) C11═C12 and C12−C13 bonds are significantly twisted in all chromophores except 13dm. (Note that the sign of the dihedral angles is irrelevant under this condition and reflects only the conformation of the chromophore in the original pocket. No chiral discrimination can result from a two-point fixation.) Additional constraints by a group of five amino acids (Thr118, Ile189, Tyr191, Met207, and Tyr268) which line the C19 methyl group, or by Trp265 and Ala117 close to the center of the chromophore chain, do not induce any significant twist in the 13dm chromophore and change the twist of the other chromophores only gradually. (We cannot rule out the possibility, however, that these groups will only support the chromophore with the "correct" helicity.) A dramatic effect is observed when the groups binding to N16 are considered. With H16, which forms the bridge between N16 and the counterion Glu113, the 13dm chromophore is twisted strongly, and in the correct direction, and the twist of the other chromophores increases except for that of 10me, which appears already strained to its limits. The same effect is observed for Lys296 which through its alkyl chain is connected to the chromophore. The next to last column shows that fixation of the nitrogen is not necessary to achieve the nonplanar chromophore conformation: with only C6 and the three backbone atoms of Lys296 held in place, the twisted geometries of the chromophores are stable and their absolute conformations are conserved.

There are two puzzling aspects concerning the stability of the 11-*cis*-retinal chromophore inside the pocket. In the dark state, the chromophore is extremely stable, with an estimated half-life of more than 420 years (*51*). At the same time, the protein exhibits an extraordinary reactivity toward light. The latter aspect has received broad attention in the past several years, and the main factors responsible for the reactivity of the chromophore have been identified: the fast movement of the excited chromophore along the torsional C11═C12 coordinate out of the Franck−Condon region coupled with an efficient nonradiative conversion to the ground state through a conical intersection (*52*−*54*). Fast torsion appears to require the pretwist of the chromophore about the C11═C12 and C12−C13 bonds; i.e., it requires a strained chromophore which, however, must be stable in the dark, or "dormant" state (*12*), of the protein to minimize the consequences of thermal noise (*55*). How is this accomplished?

The twist of the 11-*cis*-retinal chromophore results from several interactions between the protein and the chromophore, and some are identified in Table 1. Fitting the β-ionone ring into the hydrophobic pocket on one end and forming the salt bridge on the other end reduce the distance between C6 and N16 and cause the chromophore to twist about the C11═C12 bond, provided there is a methyl group at C13. The sense of twist is determined by Lys296 and by Glu113, and this is shown quite clearly in the case of the 13dm derivative. Figure 4 illustrates how these two groups which are positioned off the plane of the chromophore exert a clockwise torque on the chromophore through the planar N16 fragment. The chromophore follows this rotation until the C11═C12 bond is reached where the trans conjugation is interrupted and the twist about the cis bond separates one part of the chromophore from the other. Note that these two effects are not cumulative; they are not even additive. Lys296 and H16 induce separately a twist of −11.7° in the 13dm chromophore, while the combined effect is only −15.0°. When the chromophore is already strongly twisted by the distance constraint alone (as in 10me), torsion of the nitrogen will add little to this pretwist, and the combined effect of the environment will even reduce the twist.

Table 2 shows how point mutations affect the geometries of the 13dm and wild-type chromophores. The calculations have been performed in rhodopsin with the QM/MM method.

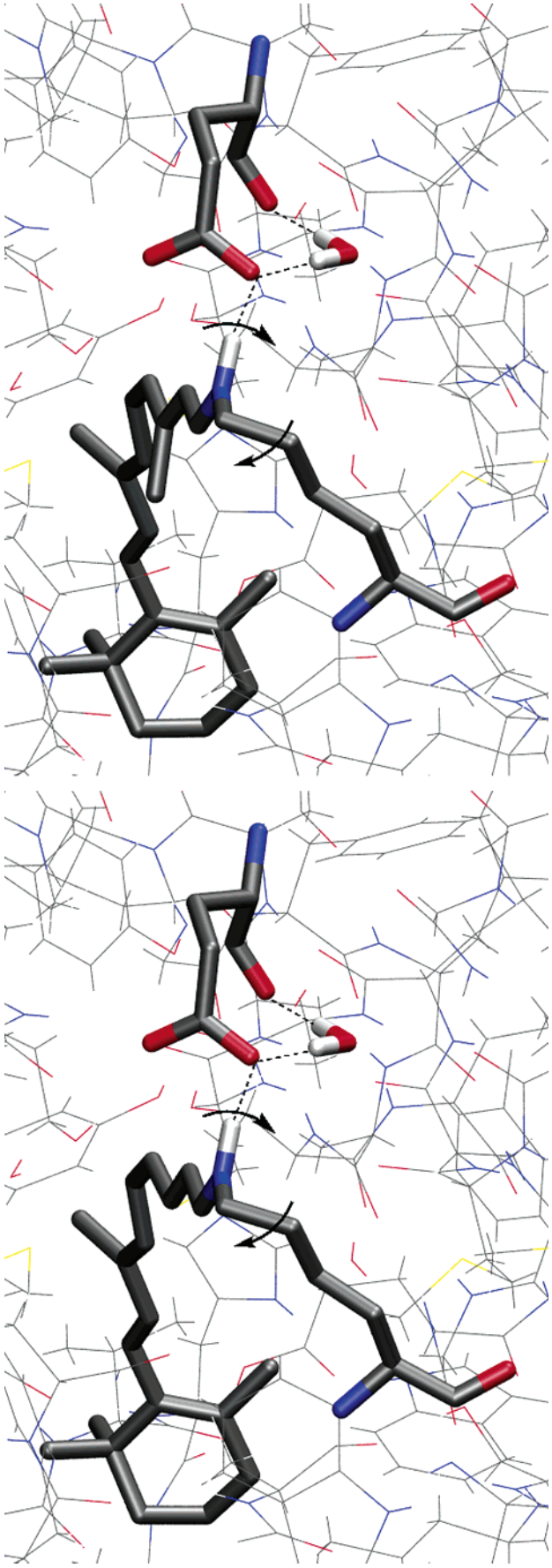

FIGURE 4: Chromophores of wild-type rhodopsin (top) and 13dm-rhodopsin (bottom) in the binding pocket. Covalently attached Lys296 and the counterion Glu113 are seen to exert clockwise torque on the plane of the N16 fragment.

Turning to 13dm-retinal first, we found substitution of Glu113 with alanine (E113A) which breaks the hydrogen bond increases the twist of the 13dm chromophore, while breaking the covalent bond with Lys296 (K296A) results in a flattened chromophore. When both the salt bridge and the covalent bond are broken (E113A/K296A), the chromophore is still twisted, which proves that the binding pocket as a whole also supports the twisted chromophore. The effect of Ala117 and Trp265 on the chromophore is rather small: substituting either of these amino acids with the shorter residues glycine and alanine (A117G and W265A, respectively) or the combined effect of both mutations does not show any significant effect. Mutations affect the wild-type chromophore in a different manner. Removing the counterion (E113A) leads to a dramatic increase of the C11═C12 bond twist to almost −30°. Obviously, the hydrogen bond in this case impedes the torsion of the chromophore which because of Lys296 is already strongly twisted. Breaking the covalent bond results in a somewhat relaxed chromophore, while the twist increases again in the double mutant. As in the 13dm derivative, the effect of A117 and W265 on the chromophore geometry is rather weak.

The picture which emerges from these calculations is that of a binding pocket which is fine-tuned to generate and preserve a particular chromophore conformation. Through several contacts, from the β-ionone ring embedded in its hydrophobic pocket to the salt bridge at the Schiff base terminus and probably many others along the polyene chain, this conformation achieves an enormous stability, until the photochemical event destroys this peace.

Rhodopsin mutants without a covalent bond between the chromophore and the protein backbone have been reported to show UV−vis spectra similar to that of the wild type and after photoexcitation even activate the G-protein with high efficiency (*56*). Similar results have been reported for bacteriorhodopsin (*57*). Our calculations support these findings: the binding pocket, through natural selection, is obviously adjusted to the chromophore and keeps it in the pretwisted conformation even when some of the restraints are no longer operative.

Optical Properties and Rotatory Strengths. For the geometries of the five chromophores inside the protein pocket, CASSCF and CASPT2 calculations have been performed to obtain the UV−vis and CD spectral data. The results are summarized in Table 3. (The complete table listing the CAS energies, the state configurations, and the components of the dipole moment is in the Supporting Information.) Comparison of the data for the different chromophores reveals that the electronic structures conform to the same pattern in each case: The ground state S_0 which is configurationally rather pure (∼75% closed shell) is followed by the first excited state S_1 with high HOMO−LUMO character (∼65%) and high oscillator strength. This "ionic" state is also characterized by a very unsymmetric charge distributution with a dipole moment of more than 18 D in all cases. The next state, S_2, is configurationally mixed, consisting of the HOMO to LUMO+1 and HOMO−1 to LUMO single excitations and of the HOMO to LUMO double excitation. This state is spectrally silent in all derivatives having neither oscillator nor rotatory strengths.

Because of the shortened chromophores, the calculated excitation energies are always higher in comparison to the

Table 3: CASPT2-Corrected State Energies E,[a] Oscillator Strengths f, Rotatory Strengths R,[b] and Dipole Moments m[c] for the Ground and Excited States of Retinal and Retinal Derivatives

chromophore	state	E	f	R	m
wild type	S_0	−670.7365			9.77
	S_1	2.86 (434)	0.89	0.66	19.1
	S_2	3.10 (400)	0.00	−0.00	9.43
13dm	S_0	−631.5552			9.41
	S_3	2.97 (418)	0.89	0.33	19.5
	S_4	3.10 (400)	0.00	−0.00	9.16
10me,13dm	S_0	−670.7308			9.42
	S_1	2.89 (430)	0.84	0.82	18.9
10me	S_0	−709.9120			9.37
	S_1	2.77 (448)	0.77	0.99	18.0
	S_3	3.01 (412)	0.00	0.00	9.08
9dm	S_0	−631.5549			9.70
	S_1	3.02 (410)	0.91	0.75	17.9
	S_2	3.22 (386)	0.00	−0.00	9.42

[a] Ground-state energies in au., excited-state energies in eV relative to the ground states and in nm (in parentheses). [b] In au. [c] In Debye.

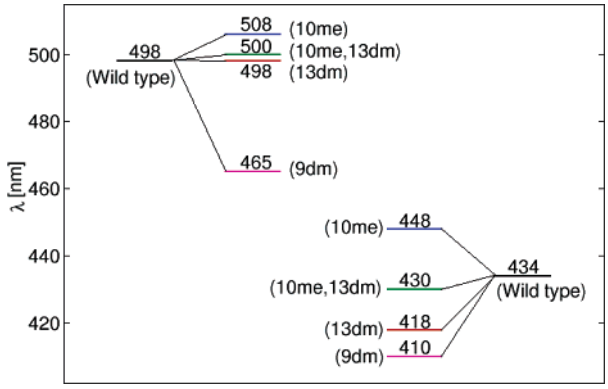

FIGURE 5: Calculated absorption maxima of retinal chromophores after relaxation within the rhodopsin binding pocket (right). For comparison, experimental data for the corresponding rhodopsin pigments are also shown (left). Data for the pigments are from ref *22* for 13dm and 10me,13dm, from ref *29* for 10me, and from ref *30* for 9dm.

experimental values. For the wild-type five-double bond chromophore, this leads to a calculated absorbance maximum of the S_1 state of 434 nm compared to the value of 498 nm found experimentally (Figure 5). Shifts of the retinal analogues relative to the wild type are, however, reproduced rather well. Thus, 10me-rhodopsin has the largest calculated (14 nm) and observed (10 nm) red shift relative to rhodopsin, while the pigment with the strongest blue shift is 9dm-rhodopsin (calculated shift of 24 nm, observed shift of 33 nm). 13dm-Rhodopsin behaves in a somewhat peculiar fashion: the calculated blue shift is 16 nm, while the corresponding pigment shows no shift at all. Finally, there is only a small blue shift for the 10me,13dm chromophore (4 nm) compared to an equally small but red shift of 2 nm for the pigment. These spectral shifts can be rationalized on the basis of two effects: torsion of double bonds leads to a red shift of ~10 nm for a 20° twist, and substitution of chain hydrogens with methyl results in a 5−10 nm red shift depending on the position and increasing with distance from the positive center (J. Hufen, unpublished results). Thus, the red shift of the 10me chromophore reflects the effect of the additional methyl substituent, while the blue shift of 9dm-retinal is the combined result of demethylation and the loss of double bond torsion relative to retinal.

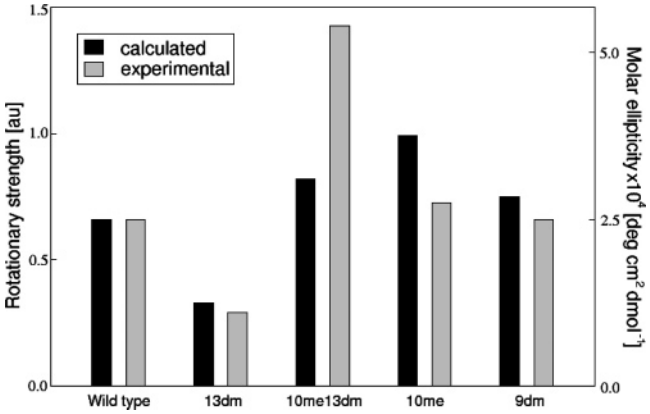

FIGURE 6: Calculated rotatory strengths of retinal chromophores vs experimental ellipticities of pigments. Experimental data are from ref *22* for 13dm and 10me,13dm, from ref *29* for 10me, and from D. Richter for 9dm.

There is a strong correlation between the oscillator strength of the S_1 state and the out-of-plane torsion of the C11═C12 bond: the strongly twisted 10me derivative has the lowest oscillator strengths of all chromophores, while 9dm-retinal has the highest, with the others between them. This correlation is plausible: in a nonplanar chromophore, the transition density between the S_0 and S_1 states is distributed not in two but in all three dimensions. Under isotropic conditions of measurement, the oscillator strength is proportionate to the square root of the sum of the squares of the different moments, and this is always larger in a planar than in any twisted conformation.

For all five chromophores, the calculated rotatory strengths (R) of the S_0 to S_1 excitation of the chromophores are positive, ranging from 0.33 for the least twisted 13dm chromophore to 0.99 au for the strongly twisted 10me chromophore. The experimental CD data for the absorbance corresponding to the S_1 state are rather scattered. Thus, for rhodopsin, $\Delta\epsilon_{max}$ values for the 500 nm band, the so called α-band, range from 3 (*58*) to 13 [calculated from the measured ellipticity (*21*)], corresponding to rotatory strengths between 0.036 and 0.136 au. We therefore have utilized data from only one laboratory (*22*, *29*) so that the effects due to different preparations, conditions of measurement, etc., may be expected to cancel. The data for 9dm-rhodopsin were provided by D. Richter from these labs. Experimental ellipticities and calculated rotatory strengths shown in Figure 6 are scaled such that data relative to wild-type rhodopsin become apparent. If the inherent twist of the chromophore about the C12−C13 bond is responsible for the CD intensity of the 500 nm band as is generally assumed following the work on torsionally restricted retinals (*59*), it appears that the calculated rotatory strengths conform more closely to the chromophore structures than the experimental values.

There is another band in the CD spectra of rhodopsin around 330 nm, the so called β-band. It corresponds probably to the excitation to one of the higher states of the chromophore which is outside the goal of these calculations.

In the following, we will discuss particular aspects of each retinal mutant with respect to the calculated properties.

Rhodopsin. Even before the first X-ray structures yielded high-resolution geometries of the whole protein, including the binding pocket, there was general agreement that the rhodopsin chromophore from C10 to C13 is significantly

twisted (*20*). Lugtenburg and co-workers, using a combination of different solid-state NMR techniques (*16*, *60*, *61*), determined an angle of approximately 44° between the planes from C7 to C10 and from C13 to C15 (*16*). Determination of the absolute sign of this angle was outside the scope of these methods and had to await experiments with an enantiomerically locked chromophore (*62*, *63*). These studies confirmed the theoretical prediction that the positive CD of the α-band of rhodopsin correlates with the negative sign of the C11═C12 dihedral angle (*64*, *65*). In the first X-ray structure of rhodopsin (*4*), the chromophore was found to be essentially planar except for the C12−C13 bond which in chain B had a dihedral angle of 157°. Later and more refined X-ray structures (*5*−*8*) gave different distributions of dihedral angles along the chain; however, they all show the C13 methyl group strongly twisted out of the plane of the chromophore, leading to negative and positive dihedral angles about the C11═C12 and C12−C13 bonds, respectively. Theoretical calculations using ab initio theory for the binding pocket (*66*) or QM/MM methodology for the whole protein (*8*, *67*, *68*) agree with respect to the absolute configuration imposed on the chromophore by the pocket, and this is also the result of our study (Figure 3). The calculated rotatory strength for the rhodopsin model chromophore agrees in sign and magnitude with the results obtained for the complete chromophore (M. Schreiber; unpublished results).

13dm-Rhodopsin. With the C13 methyl group missing, the out-of-plane torsion of the chromophore in the binding pocket as measured by the C7−C10/C13−C15 interplane angle is significantly reduced, from 31° in the wild type to −2° in the 13dm analogue. The flattening of the chromophore which we see in the calculations is reflected in the weaker CD α-band which is reduced in magnitude to less than half compared to that of rhodopsin both in the spectra and in the calculations. However, torsion of the C11═C12 bond in 13dm-rhodopsin persists; it is almost as strong as in the wild type (−15.1° vs −18.2°). This appears to contradict RR spectroscopic evidence which with its reduced intensity of the HC_{11}═$C_{12}H$ hydrogen out-of-plane vibration indicates reduction of the C11═C12 torsion (*22*). Experimental values for the quantum yield of this analogue range from 0.3 (*26*) to 0.47 (*22*, *25*), so the photoconversion to the batho state is still quite effective. This we take as supporting evidence for the calculated structure with its significant pretwist of the C11═C12 bond.

10me,13dm-Rhodopsin. According to the calculations, this chromophore is already strongly twisted outside the binding pocket; in the pocket, the twisting pattern of the polyene chain is similar to that of the wild type, leading to a very similar value of the overall twist of the chromophore. Thus, the idea (*22*, *27*) of reintroducing the strain into the chromophore of 13dm-rhodopsin, albeit at another position, seems to work quite nicely. Unfortunately, there is wide divergence of the experimentally determined quantum efficiencies of this rhodopsin mutant. So the question of whether an efficient photoreaction needs not only the pretwist of the chromophore but also the C13 methyl group must still be considered to be unresolved.

10me-Rhodopsin. Direct experimental evidence for increased out-of-plane distortion of this chromophore has been obtained from internuclear distance measurements using solid-state NMR spectroscopy (*61*). It was found, among others, that the C10−C20 distance in 10me-rhodopsin increases as a consequence of the added 10-methyl group, from 3.04 ± 0.15 to 3.47 ± 0.15 Å. Our calculated values are 2.55 and 2.97 Å, respectively, which are shorter but show the same relative increase. Indirect evidence for increased torsion in this chromophore comes from UV−vis spectroscopy: the α-band absorbance (ϵ_{max} = 24 000) is significantly smaller compared to that of the wild type (40 000) (*29*). This agrees with the reduced oscillator strength which we calculate for this excitation (0.77 in 10me-rhodopsin vs 0.89 in the wild type). As a consequence of the strongly distorted chromophore, the calculated rotatory strength is significantly larger than in the wild type, a result which is not borne out by the experiment where practically identical CD intensities are obtained for the two rhodopsins (*29*). The strong distortion of the 10me-retinal chromophore does not prevent its binding by the protein where, however, its geometry is adjusted to the constraints provided by the pocket. While the quantum yield of photoconversion to the batho stage, 0.55 (*29*), is almost as high as in the wild type, the additional methyl group interferes in the following stages, apparently by extra stabilization of the batho stage and interference with the transitions leading to the signaling state (*29*).

9dm-Rhodopsin. The absorbance of this pigment is strongly blue-shifted relative to that of the wild type (*69*), contributors to this shift being the increased planarity of the chromophore and the removal of a methyl group distant from the nitrogen. The small opsin shift of only 1700 cm^{-1} indicates the less than perfect fit with the protein pocket. The position of the C9 methyl group is almost identical in the different pigments which indicates strong steric interaction with the pocket, in particular, Thr118, Tyr191, and Tyr268. The O−H stretching vibration of Thr118 has been identified by FTIR spectroscopy, suggesting that this residue is located at a crucial position in the interaction with the retinal chromophore (*70*). The 9-methyl group is important for activation of the protein, and it is known that a clear batho intermediate cannot be detected in its photocascade (*71*).

CONCLUSIONS

On the basis of the rhodopsin crystal structure, we have calculated the conformations and optical properties of retinal and of four retinal analogues in rhodopsin. We have identified two constraints which determine the shape of the chromophore inside the binding pocket. Fitting the β-ionone ring into its binding pocket at one end and forming the salt bridge at the other impose a distance constraint on the chromophore, reducing the C6−N16 distance in rhodopsin from 11.51 to 11.19 Å. The second constraint is exerted through the counterion Glu113 and Lys296. With both of them positioned off the plane of the chromophore, their bonds to N16 exert a clockwise torque on the chromophore, leading to the negative dihedral angle of the C11═C12 bond. These constraints combined with a protein pocket adjusted to the twisted chromophore conformation render the rhodopsin molecule exceedingly stable in the dark. Calculated optical and chiroptical properties of the retinal analogues are in general agreement with experimental data.

ACKNOWLEDGMENT

All computations were performed at the Computational Center of the University of Duisburg-Essen and at the Regional Computational Center of the University of Cologne (Cologne, Germany).

SUPPORTING INFORMATION AVAILABLE

Detailed information about the structures described in this work, including Cartesian coordinates of all minimized chromophores inside and outside the protein pocket and a table listing the CAS energies, the state configurations, and the components of the dipole moments. This material is available free of charge via the Internet at http://pubs.acs.org.

REFERENCES

1. Sprang, S. R. (1997) G protein mechanisms: Insight from structural analysis, *Annu. Rev. Biochem. 66*, 639−678.
2. Ballesteros, J. A., Shi, L., and Javitch, J. A. (2001) Structural mimicry in G protein-coupled receptors: Implications of the high-resolution structure of rhodopsin for structure−function analysis of rhodopsin-like receptors, *Mol. Pharmacol. 60*, 1−19.
3. Okada, T., Trong, I. L., Fox, B. A., Behnke, C. A., Stenkamp, R. E., and Palczewski, K. (2000) X-ray diffraction analysis of three-dimensional crystals of bovine rhodopsin obtained from mixed micelles, *J. Struct. Biol. 130*, 73−80.
4. Palczewski, K., Kumasaka, T., Hori, T., Behnke, C. A., Motoshima, H., Fox, B. A., Le Trong, I., Teller, D. C., Okada, T., Stenkamp, R. E., Yamamoto, M., and Miyano, M. (2000) Crystal structure of rhodopsin: A G-protein-coupled receptor, *Science 289*, 739−745.
5. Teller, D. C., Okada, T., Behnke, C. A., Palczewski, K., and Stenkamp, R. E. (2001) Advances in determination of a high-resolution three-dimensional structure of rhodopsin, a model of G-protein-coupled receptors (GPCRs), *Biochemistry 40*, 7761−7777.
6. Okada, T., Fujiyoshi, Y., Silow, M., Navarro, J., Landau, E. M., and Shichida, Y. (2002) Function role of internal water molecules in rhodopsin revealed by X-ray crystallography, *Proc. Natl. Acad. Sci. U.S.A. 99*, 5982−5987.
7. Li, J., Edwards, P. C., Burghammer, M., Villa, C., and Schertler, G. F. X. (2004) Structure of bovine rhodopsin in a trigonal crystal form, *J. Mol. Biol. 343*, 1409−1438.
8. Okada, T., Sugihara, M., Bondar, A.-N., Elstner, M., Entel, P., and Buss, V. (2004) The retinal conformation and its environment in rhodopsin in light of a new 2.2 Å crystal structure, *J. Mol. Biol. 342*, 571−583.
9. Sugihara, M., Buss, V., Entel, P., and Hafner, J. (2004) The nature of the complex counterion of the chromophore in rhodopsin, *J. Phys. Chem. B 108*, 3673−3680.
10. Spooner, P. J. R., Sharples, J. M., Goodall, S. C., Bovee-Geurts, P. H. M., Verhoeven, M. A., Lugtenburg, J., Pistorius, A. M. A., DeGrip, W. J., and Watts, A. (2004) The ring of the rhodopsin chromophore in a hydrophobic activation switch within the binding pocket, *J. Mol. Biol. 343*, 719−730.
11. Hubbard, R. (1969) Absorption spectrum of rhodopsin: 500 nm absorption band, *Nature 221*, 432−435.
12. Okada, T., Ernst, O. P., Palczewski, K., and Hofmann, K. P. (2001) Activation of rhodopsin: New insights from structural and biochemical studies, *Trends Biochem. Sci. 26*, 318−324.
13. Yoshizawa, T., and Wald, G. (1963) Pre-lumirhodopsin and the bleaching of visual pigments, *Nature 197*, 1279−1286.
14. Hofmann, K. P. (2000) Late photoproducts and signalling states of bovine rhodopsin, in *Molecular mechanisms of visual transduction* (Stavenga, D. G., Degrip, W. J., and Pugh, E. N., Jr., Eds.) pp 91−145, Elsevier, Amsterdam.
15. Smith, S. O., Palings, I., Copié, V., Raleigh, D. P., Courtin, J., Pardoen, J. A., Lugtenburg, J., Mathies, R. A., and Griffin, R. G. (1987) Low-temperature solid-state ^{13}C NMR studies of the retinal chromophore in rhodopsin, *Biochemistry 26*, 1606−1611.
16. Mathies, R. A., and Lugtenburg, J. (2000) The primary photoreaction of rhodopsin, in *Molecular mechanisms in visual transduction* (Stavenga, D. G., DeGrip, W. J., and Pugh, E. N., Jr., Eds.) pp 55−90, Elsevier, Amsterdam.
17. Carravetta, M., Zhao, X., Johannesen, O. G., Lai, W. C., Verhoeven, M. A., Bove-Geurths, P. H. M., Verdegem, P. J. E., Kiihne, S., Luthman, H., de Grot, H. J. M., deGrip, W. J., Lugtenburg, J., and Levitt, M. E. (2004) Protein-induced bonding perturbation of the rhodopsin chromophore detected by double-quantum solid-state NMR, *J. Am. Chem. Soc. 126*, 3948−3953.
18. Salgado, G. F. J., Struts, A. V., Tanaka, K., Fujioka, N., Nakanishi, K., and Brown, M. F. (2004) Deuterium NMR structure of retinal in the ground state of rhodopsin, *Biochemistry 43*, 12819−12828.
19. Palings, I., Pardoen, J. A., van den Berg, E., Winkel, C., Lugtenburg, J., and Mathies, R. A. (1987) Assignment of fingerprint vibrations in the resonance Raman spectra of rhodopsin, isorhodopsin, and bathorhodopsin: Implications for chromophore structure and environment, *Biochemistry 26*, 2544−2556.
20. Lin, S. W., Groesbeek, M., van der Hoef, I., Verdegem, P., Lugtenburg, J., and Mathies, R. A. (1998) Vibrational assignment of torsional normal modes of rhodopsin: Probing excited-state isomerization dynamics along the reactive C_{11}═C_{12} torsion coordinate, *J. Phys. Chem. B 102*, 2787−2806.
21. Waggoner, A. S., and Stryer, L. (1971) Induced optical activity of the metarhodopsins, *Biochemistry 10*, 3250−3254.
22. Kochendoerfer, G. G., Verdegem, P. J. E., van der Hoef, I., Lugtenburg, J., and Mathies, R. A. (1996) Retinal analog study of the role of steric interactions in the excited-state isomerization dynamics of rhodopsin, *Biochemistry 35*, 16230−26240.
23. Terstegen, F., and Buss, V. (1996) All-trans- and 11-cis-retinal, their *N*-methyl Schiff base and *N*-methyl protonated Schiff base derivatives: A comparative ab initio study, *THEOCHEM 369*, 53−65.
24. Terstegen, F., and Buss, V. (1998) Influence of DFT-calculated electron correlation on energies and geometries of retinals and of retinal derivatives related to the bacteriorhodopsin and rhodopsin chromophores, *THEOCHEM 430*, 209−218.
25. Wang, Q., Kochendoerfer, G. G., Schoelein, R. W., Verdegem, P. J. E., Lugtenburg, J., Mathies, R. A., and Shank, C. V. (1996) Femtosecond spectroscopy of a 13-demethylrhodopsin visual pigment analogue: The role of nonbonded interactions in the isomerization process, *J. Phys. Chem. 100*, 17388−17394.
26. Gärtner, W., and Ternieden, S. (1996) Influence of a steric hindrance in the chromophore of rhodopsin on the quantum yield of the primary photochemistry, *J. Photochem. Photobiol., B 33*, 83−86.
27. Koch, D., and Gärtner, W. (1997) Steric hindrance between chromophore substituents as the driving force of rhodopsin photoisomerization: 10-Methyl-13-demethyl retinal containing rhodopsin, *Photochem. Photobiol. 65*, 181−186.
28. Schoenlein, R. W., Peteanu, L. A., Wang, Q., Mathies, R. A., and Shank, C. V. (1993) Femtosecond dynamics of cis−trans isomerization in a visual pigment analog: Isorhodopsin, *J. Phys. Chem. 97*, 12087−12092.
29. DeLange, F., Bovee-Geurts, P. H. M., VanOostrum, J., Portier, M. D., Verdegem, P. J. E., Lugtenburg, J., and DeGrip, W. J. (1998) An additional methyl group at the 10-position of retinal dramatically slows down the kinetics of the rhodopsin photocascade, *Biochemistry 37*, 1411−1420.
30. Han, M., Groesbeek, M., Smith, S. O., and Sakmar, T. P. (1998) Role of the C_9 methyl group in rhodopsin activation: Characterization of mutant opsins with the artificial chromophore 11-*cis*-9-demethylretinal, *Biochemistry 37*, 538−545.
31. MacKerell, A. D., Jr., Bashford, D., Bellott, M., Dunbrack, R. L., Jr., Evanseck, J. D., Field, M. J., Fischer, S., Gao, J., Guo, H., Ha, S., Joseph-McCarthy, D., Kuchnir, L., Kuczera, K., Lau, F. T. K., Mattos, C., Michnick, S., Ngo, T., Nguyen, D. T., Prodhom, D., Reiher, W. E., III, Roux, B., Schlenkrich, M., Smith, J. C., Stote, R., Straub, J., Watanabe, M., Wiórkiewicz-Kuczera, J., Yin, D., and Karplus, M. (1998) All-atom empirical potential for molecular modeling and dynamics studies of proteins, *J. Phys. Chem. B 102*, 3586−3616.
32. Buss, V., Sugihara, M., Entel, P., and Hafner, J. (2003) Thr94 and Wat2b effect protonation of the retinal chromophore in rhodopsin, *Angew. Chem., Int. Ed. 42*, 3245−3247.
33. Crozier, P. S., Stevens, M. J., Forrest, L. R., and Woolf, T. B. (2003) Molecular dynamics simulation of dark-adapted rhodopsin in an explicit membrane bilayer: Coupling between local retinal and large scale conformational change, *J. Mol. Biol. 333*, 493−514.
34. Cui, Q., Elstner, M., Kaxiras, E., Frauenheim, T., and Karplus, M. (2001) A QM/MM implementation of the self-consistent charge

density functional tight binding (SCC-DFTB) method, *J. Phys. Chem. B 105*, 569−585.
35. Bondar, A.-N., Fischer, S., Smith, J. C., Elstner, M., and Suhai, S. (2004) Key role of electrostatic interactions in bacteriorhodopsin proton transfer, *J. Am. Chem. Soc. 126*, 14668−14677.
36. Bondar, A.-N., Fischer, S., Suhai, S., and Smith, J. C (2005) Tuning of retinal twisting in bacteriorhodopsin controls the directionality of the early photocycle steps, *J. Phys. Chem. B 109*, 14786−14788.
37. Nosé, S. (1984) A unified formulation of the constant temperature molecular dynamics methods, *J. Chem. Phys. 81*, 511−519.
38. Andersson, K., Baryz, M., Bernhardsson, A., Blomberg, M. R. A., Cooper, D. L., Fülscher, M. P., de Graaf, C., Hess, B., Karlström, G., Lindh, R., Malmqvist, P.-Å., Nakajima, T., Neogrady, P., Olsen, J., Roos, B. O., Schimmelpfennig, B., Schütz, M., Seijo, L., Serrano-Andres, L., Siegbahn, P. E., Stålring, J., Thorsteinsson, T., Veryazov, V., and Widmark, P.-O. (2002) *Molcas*, version 5.4, Department of Theoretical Chemistry, Chemistry Center, University of Lund, S-22100 Lund, Sweden.
39. Malmqvist, P.-Å., and Roos, B. O. (1989) The CASSCF state interaction method, *Chem. Phys. Lett. 155*, 189−194.
40. Schreiber, M., and Buss, V. (2003) Origin of the bathochromic shift in the early photointermediates of the rhodopsin visual cycle: A CASSCF/CASPT2 study, *Int. J. Quantum Chem. 95*, 882−889.
41. Schreiber, M., Buss, V., and Sugihara, M. (2003) Exploring the opsin shift with ab initio methods: Geometry and counterion effects on the electronic spectrum of retinal, *J. Chem. Phys. 119*, 12045−12048.
42. Ferré, N., and Olivucci, M. (2003) Probing the rhodopsin cavity with reduced retinal model at the CASPT2//CASSCF/AMBER level of theory, *J. Am. Chem. Soc. 125*, 6868.
43. Andruniów, T., Ferré, N., and Olivucci, M. (2004) Structure, initial excited-state relaxation, and energy storage of rhodopsin resolved at the multiconfigurational perturbation theory level, *Proc. Natl. Acad. Sci. U.S.A. 101*, 17908−17913.
44. Wanko, M., Hoffmann, M., Strodel, P., Koslowski, A., Thiel, W., Neese, F., Frauenheim, T., and Elstner, M. (2005) Calculating absorption shifts for retinal proteins: Computational challenges, *J. Phys. Chem. B 109*, 3606−3615.
45. Hufen, J., Sugihara, M., and Buss, V. (2004) How the counterion affects the optical ground- and excited-state properties of the rhodopsin chromophore, *J. Phys. Chem. B 108*, 20419−20426.
46. Buss, V., Weingart, O., and Sugihara, M. (2000) Fast photoisomerization of a rhodopsin chromophore model: An ab initio molecular dynamics study, *Angew. Chem., Int. Ed. 39*, 2784−2786.
47. Bifone, A., de Groot, H. J. M., and Buda, F. (1997) Ab initio molecular dynamics of rhodopsin, *Pure Appl. Chem. 69*, 2105−2110.
48. Bifone, A., de Groot, H. J. M., and Buda, F. (1997) Energy storage in the primary photoproduct of vision, *J. Phys. Chem. B 101*, 2954−2958.
49. Sugihara, M., Entel, P., and Buss, V. (2002) A first principles study of 11-cis-retinal: Modelling the chromophore−protein interaction in rhodopsin, *Phase Transitions 75*, 11−17.
50. Liu, S. H. L., and Mirzagedan, T. (1988) The shape of a three-dimensional binding site of rhodopsin based on molecular modelling analyses of isomeric and other visual pigment analogues, *J. Am. Chem. Soc. 110*, 8617−8623.
51. Schnapf, J., and Baylor, D. A. (1987) How photoreceptr cells respond to light, *Sci. Am. 256*, 32−39.
52. González-Luque, R., Garavelli, M., Bernardi, F., Merchán, M., Robb, M. A., and Olivucci, M. (2000) Computational evidence in favor of a two-state, two-model of the retinal chromophore photoisomerization, *Proc. Natl. Acad. Sci. U.S.A. 97*, 9379−9384.
53. Weingart, O., Buss, V., and Robb, M. (2004) Excited-state molecular dynamics of retinal model chromophore, *Phase Transitions 78*, 17−24.
54. Weingart, O., Migani, A., Olivucci, M., Robb, M. A., Buss, V., and Hunt, P. (2004) Probing the photochemical functional of a retinal chromophore model via zero-point energy sampling semiclassical dynamics, *J. Phys. Chem. A 108*, 4685−4693.
55. Barlow, R. B., Birge, R. R., Kaplan, E., and Tallent, J. R. (1993) On the molecular origin of photoreceptor noise, *Nature 366*, 64−66.
56. Zhukovsky, E. A., Robinson, P. R., and Oprian, D. D. (1991) Transducin activation by rhodopsin without a covalent bond to the 11-cis-retinal chromophore, *Science 251*, 558−560.
57. Friedman, N., Druckmann, S., Lanyi, J., Needleman, R., Lewis, A., Ottolenghi, M., and Sheves, M. (1994) A covalent link between the chromophore and the protein backbone of bacteriorhodopsin is not required for forming a photochemically active pigment analogous to the wild type, *Biochemistry 33*, 1971−1976.
58. Tan, Q., Lou, J., Borhan, B., Karnaukhova, E., Berova, N., and Nakanishi, K. (1997) Absolute sense of twist of the C12−C13 bond of the retinal chromophore in bovine rhodopsin based on exiton-coupled CD spectra of 11,12-dihydroretinal analogues, *Angew. Chem., Int. Ed. 36*, 2089−2093.
59. Wada, A., Sakai, M., Imamoto, Y., Shichida, Y., Yamauchi, M., and Ito, M. (1997) Synthesis of (11*Z*)-8,18-ethanoretinal and a conformational study of the rhodopsin chromophore, *J. Chem. Soc., Perkin Trans. 1*, 1773−1777.
60. Feng, X., Verdegem, P. J. E., Lee, Y. K., Sandström, D., Edén, M., Bovee-Geurts, P., de Grip, W. J., Lugtenburg, J., de Groot, H. J. M., and Levitt, M. H. (1997) Direct determination of a molecular torsional angle in the membrane protein rhodopsin by solid-state NMR, *J. Am. Chem. Soc. 119*, 6853−6857.
61. Verdegem, P. J. E., Bovee-Geurts, P. H. M., de Grip, W. J., Lugtenburg, J., and de Groot, H. J. M. (1999) Retinylidene ligand structure in bovine rhodopsin, metarhodopsin-I, and 10-methyl-rhodopsin from internuclear distance measurements using ^{13}C-labelling and 1-D rotational resonance MAS NMR, *Biochemistry 38*, 11316−11324.
62. Fujimoto, Y., Ishihara, J., Maki, S., Fujioka, N., Wang, T., Furuta, T., Fishkin, N., Borhan, B., Berova, N., and Nakanishi, K. (2001) On the bioactive conformation of the rhodopsin chromophore. Absolute sense of twist around the 6-s-cis bond, *Chem.—Eur. J. 19*, 4198−4204.
63. Fujimoto, Y., Fishkin, N., Pescitelli, G., Decatur, J., Berova, N., and Nakanishi, K. (2002) Solution and biologically relevant conformations of enantiomeric 11-cis-locked cyclopropyl retinals, *J. Am. Chem. Soc. 124*, 7294−7302.
64. Buss, V., Kolster, K., Terstegen, F., and Vahrenhorst, R. (1998) Absolute sense of twist of the C12−C13 bond of the retinal chromophore in rhodopsin: Semiempirical and nonempirical calculations of chiroptical data, *Angew. Chem., Int. Ed. 37*, 1893−1895.
65. Buss, V. (2001) Inherent chirality of the retinal chromophiore in rhodopsin: A nonempirical theoretical analysis of chiroptical data, *Chirality 13*, 13−23.
66. Sugihara, M., Buss, V., Entel, P., Elstner, M., and Frauenheim, T. (2002) 11-cis-Retinal protonated Schiff base: Influence of the protein environment on the geometry of the rhodopsin chromophore, *Biochemistry 41*, 15259−15266.
67. Roehrig, U., Guidoni, L., Frank, I., and Rothlisberger, U. (2004) A molecular spring for vision, *J. Am. Chem. Soc. 126*, 15328−15329.
68. Gascon, J. A., and Batista, V. S. (2004) QM/MM study of the energy storage and the molecular rearrangement due to the primary event in vision, *Biophys. J. 87*, 2931−2941.
69. Kropf, A., Whittenberger, B. P., Goff, S. P., and Waggoner, A. S. (1973) The spectral properties of some visual pigment analogs, *Exp. Eye Res. 17*, 591−606.
70. Nagata, T., Oura, T., Terakita, A., Kandori, H., and Shichida, Y. (2002) Isomer-Specific Interaction of the Retinal Chromophore with Threonine-118 in Rhodopsin, *J. Phys. Chem. A 106*, 1969−1975.
71. Ganter, U. M., Schmid, E. E., Perez-Sala, D., Rando, R. R., and Siebert, F. (1989) Removal of the 9-methyl group of retinal inhibits signal transduction in the visual process. A Fourier transform infrared and biochemical investigation, *Biochemistry 28*, 5955−5972.

BI0515624